A Low-Cost Wearable Flexible Sensor with an Ag-hBN Interface for Respiratory Monitoring

Tasnim Zaman Adry, Sabiha Sharmin, Syed Kamrul Islam, and Mohammad Rafiqul Haider
Department of Electrical Engineering and Computer Science
University of Missouri-Columbia
Columbia, MO, USA
{tzfft, sabiha.sharmin, islams, mhaider}@missouri.edu

***Abstract*—Flexible sensors fabricated via inkjet-printing offer a scalable, low-cost approach for wearable health monitoring applications. In this work, a highly responsive breath sensor is demonstrated based on interdigitated silver (Ag) electrodes printed on a PET substrate using a Voltera V-One PCB printer, strategically functionalized with hexagonal boron nitride (hBN) nanoparticles at the electrode interface. Systematic testing reveals that the addition of h-BN enhances current conduction compared to pure Ag electrodes, attributed to improved interfacial charge transfer properties. The optimized sensor exhibits distinct, reproducible current profiles during inhalation and exhalation cycles, enabling real-time monitoring of respiration patterns. Comprehensive characterization through high-resolution digital microscopy, sensitive LCR measurements, and COMSOL Multiphysics® simulations demonstrates h-BN's critical role in modulating electric field distribution and boosting sensitivity. This mechanically robust, inkjet-printed platform, with a low production cost, shows significant promise for wearable respiratory monitoring in both clinical settings and fitness applications, offering advantages in scalability and performance over conventional approaches.**

***Index Terms*—Flexible Sensors, Hexagonal Boron Nitride, Inkjet-Printing, Silver Nanoparticles, Wearable Electronics.**

I. Introduction

The need for reliable respiratory monitoring systems has increased due to the increase in respiratory conditions such as asthma, sleep apnea, and chronic obstructive pulmonary disease [1]. In clinical settings, traditional spirometry is the gold standard, but it lacks portability and real-time monitoring [2]. The growth of personalized health tracking has driven the demand for wearable sensors that provide accurate respiratory data outside labs [3]. Current wearables often use rigid components or complex manufacturing, compromising comfort, sensitivity, and manufacturability [4]. Flexible electronics offer a promising alternative, but challenges persist in developing sensors with high performance and durability for long-term use [5].

Inkjet-printing technology is emerging as a viable method for flexible sensors, offering scalability, material efficiency, and design flexibility over traditional lithography [6]–[10]. However, the adoption of inkjet-printed (iJP) respiratory sensors is hindered by material challenges at key interfaces [11], [12]. Although silver nanoparticle inks are favored for conductivity, they face issues with oxidation and poor charge transfer with dielectrics [13]. Research has explored various nanomaterial additives to address these issues [14], yet hexagonal boron nitride (h-BN) - known for its thermal stability, electrical insulation, and mechanical strength - is still underused in printed flexible sensors [15]. This presents a significant opportunity to explore novel material combinations that could enhance the performance of wearable respiratory monitoring [16].

This work presents an iJP flexible respiratory sensor with a silver-hexagonal boron nitride (Ag-hBN) nanocomposite interface as shown in Fig. 1. hBN nanoparticles enhance sensor performance by protecting against silver oxidation [17], improving interfacial adhesion [18], and modulating the electrical field for better strain sensitivity [19]. Fabricated using a Voltera V-One conductive ink printer, our optimized sensor design demonstrates exceptional responsiveness to humidity changes caused by exhaled breath, enabling precise respiratory monitoring. Systematic evaluation reveals distinct and reproducible electrical signatures corresponding to various respiratory patterns. The sensor's performance stems from the synergistic combination of inkjet-printing precision and the carefully engineered Ag-hBN interface, representing a significant advancement in printable flexible electronics.

The rest of the letter is structured as follows. While Section II describes the inkjet-printing fabrication process, Section III presents the optimized breathing sensor design, followed by experimental results for respiratory patterns in Section IV. Section V provides comprehensive characterization through high-resolution digital microscopy analysis, sensitive LCR measurement results, and COMSOL Multiphysics® simulation studies that validate sensor performance. The letter is finally concluded in Section VI.

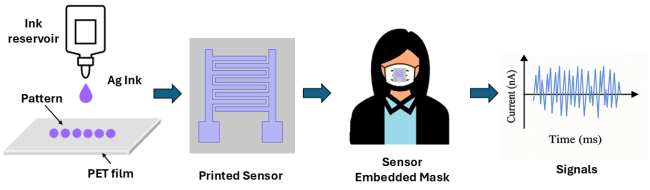

Fig. 1. Schematic illustration of the printed sensor embedded in a mask, showing the ink reservoir and Ag ink pattern on PET film.

Thanks to USA National Science Foundation (NSF), Award No. ECCS-2430440.

II. INKJET-PRINTED FABRICATION TECHNOLOGY

Inkjet-printing technology uses piezoelectric actuation to accurately deposit functional nanomaterial inks on flexible substrates, facilitating advanced wearable sensor fabrication. This emerging manufacturing paradigm offers unique advantages for biomedical applications, including design flexibility, roll-to-roll compatibility, and cost-effective prototyping of multifunctional devices [20]. As demonstrated in Fig. 2, the iJP process follows a systematic approach well-established in recent literature, though optimized here for respiratory monitoring applications [21]–[24]. The fabrication process combines iJP silver electrodes with precisely deposited hexagonal boron nitride (h-BN) interfaces.

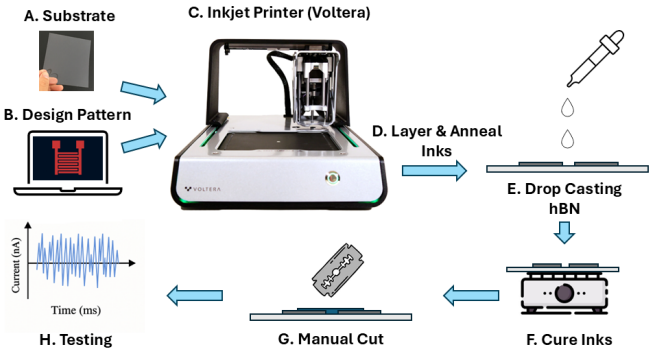

Fig. 2. The inkjet-printing fabrication process involves digital pattern design, ink layer deposition, drop casting, and functional testing.

First, interdigitated electrode patterns are printed onto flexible PET substrates using a commercially available conductive silver ink. The printed structures are thermally cured to ensure robust conductivity while preserving substrate flexibility. After electrode fabrication, a carefully prepared hBN dispersion is drop-cast at the critical electrode junctions, forming a thin interfacial layer that enhances sensor performance. To optimize the interface properties, we then introduce a controlled manual cut in the hBN layer using a precision microblade under optical guidance. This strategic cut enhances the interfacial effects by locally modifying the electric-field distribution while maintaining the overall integrity of the dielectric layer.

III. iJP BREATHING SENSOR DESIGN

Interdigitated silver (Ag) nanoparticle plates printed on a PET film substrate make up the breathing sensor, as seen in Fig. 3. Printing is done using a Voltera V-One drop-on-demand piezoelectric printer. To reduce the possibility of short circuits brought on by ink splash, the electrode gap is adjusted to roughly 0.5 mm, which is greater than the printer's minimum resolution of 0.3 mm. After printing, the ink is annealed at 70 °C for 10 minutes to improve conductivity.

The 135 μm thick PET substrate (NB-TP-3GU100, Mitsubishi Paper Mills) costs about $180 for 100 sheets. The production cost per sensor is estimated at $2.25, based on silver nanoparticle ink at $100 per cartridge (Voltera Conductor 3 – Silver Ink, 150 prints/cartridge), $1.80 per substrate

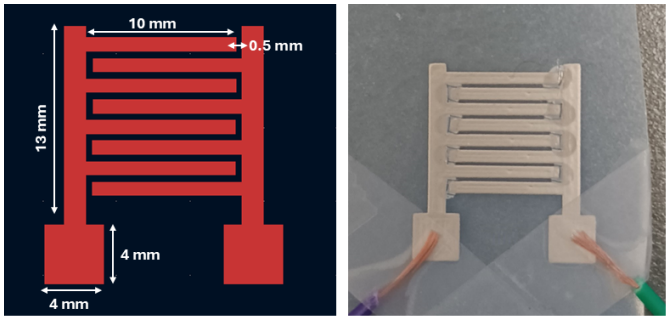

Fig. 3. Breathing sensor pattern is shown with all relevant dimensions. The structure designed in KiCAD software (left) and the printed sensor with hBN and cut (right).

sheet (150 sensor/sheet), and additional hBN ink at $200. The costs of the printer and ink dispenser are one-time expenses and excluded from this calculation.

The silver prints have a shelf life of more than two years, with degradation indicated by reduced conductivity as a result of prolonged exposure. The sensing behavior is unaffected, but the biasing of the device is affected. Hot and humid environments can also affect the sensor's biasing without affecting the sensing performance. To enhance signal reliability before clinical trials, it is recommended to use moisture- and temperature-resistant ink layers, polymer encapsulation, and EMI shielding.

IV. SENSOR DATA COLLECTION AND ANALYSIS

The breathing sensor was integrated into a face mask (see Fig. 4) and connected to a Keithley 2400 Source Meter to measure current responses under 5 V applied voltage. Fig. 5 presents the current-voltage (I–V) characteristics of the inkjet-printed breath sensor, comparing performance with and without the addition of the hBN interfacial layer. In the left plot, the sensor with only Ag electrodes shows relatively lower current values, indicating higher resistance at the electrode junctions. Upon integration of hBN (right plot), a marked increase in current response is observed across the same voltage range. This enhancement is attributed to the improved interfacial charge transport facilitated by the hBN layer, which modulates the local electric field and reduces the effective contact resistance.

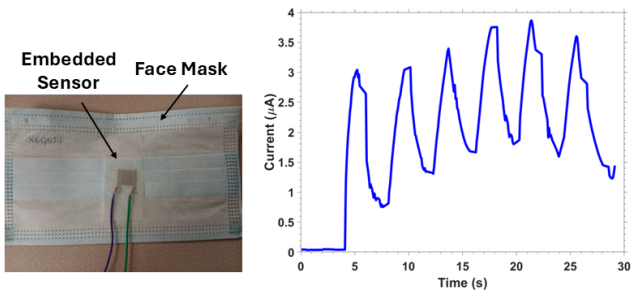

Fig. 4. The procedure for collecting data. Data is collected from the source meter while the iJP Breathing Sensor is concealed by a face mask.

As shown in Fig. 6, the current waveforms demonstrated clear breathing signals, with inhalation and exhalation, confirming the sensor's capability for respiratory monitoring with ultra-low-power consumption (<30 μW). The sensor demonstrates stable operation over extended periods without reaching saturation. Additionally, its low-cost fabrication and robust design allow it to function effectively as a disposable breathing sensor for single-use or short-term applications.

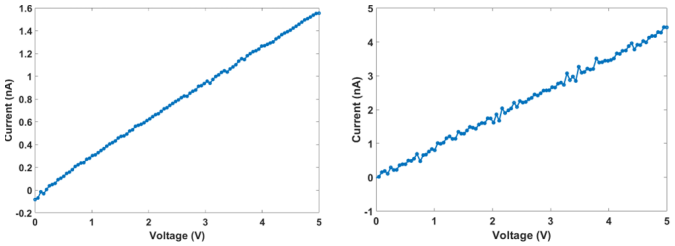

Fig. 5. I-V curve of the breath sensor without hBN layer (left) and after adding hBN layer (right).

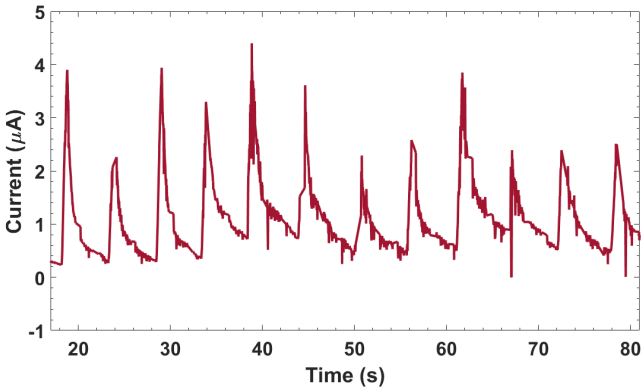

Fig. 6. Current response from the breath sensor.

V. SENSOR CHARACTERIZATION

High-resolution digital microscopy characterized the interfacial morphology of the Ag-hBN sensor, revealing critical structural features as shown in Fig. 7. The images confirmed a uniform deposition of hBN at the electrode junctions. The post-cycling inspection after mechanical testing showed no visible cracking or delamination, verifying the structural integrity of the drop-cast hBN interface under operational stresses.

Sensitive LCR measurements quantified the electrical enhancement of the integration of hBN. The impedance and capacitance spectra of the sensor are shown in Fig. 8. Impedance spectroscopy (10 Hz–10 MHz) demonstrated an increase in capacitance sensitivity compared to pure Ag electrodes under identical respiratory stimuli. These measurements were correlated with the sensor's superior current response, showing a lower signal drift during prolonged operation.

The impedance magnitude ($|Z|$) decreases monotonically from $\sim 10^7$ Ω at low frequencies (1–100 Hz) to $\sim 10^2$ Ω at high frequencies (>1 MHz), following the characteristic trend:

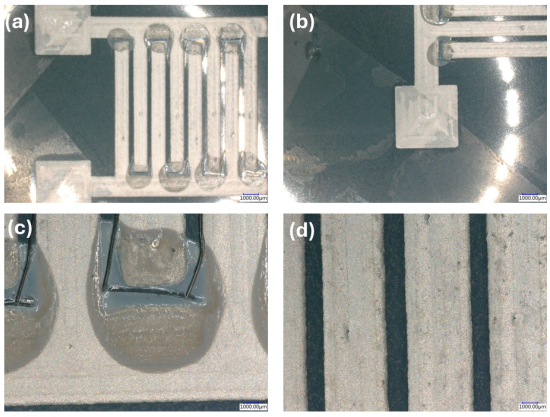

Fig. 7. Microscopic characterization of inkjet-printed flexible sensor: (a) Full sensor layout showing the integrated components, (b) Contact pad region illustrating the conductive ink deposition quality, (c) Ag-hBN interfacial region critical for dielectric performance, and (d) High-magnification of the electrodes for demonstrating printing precision.

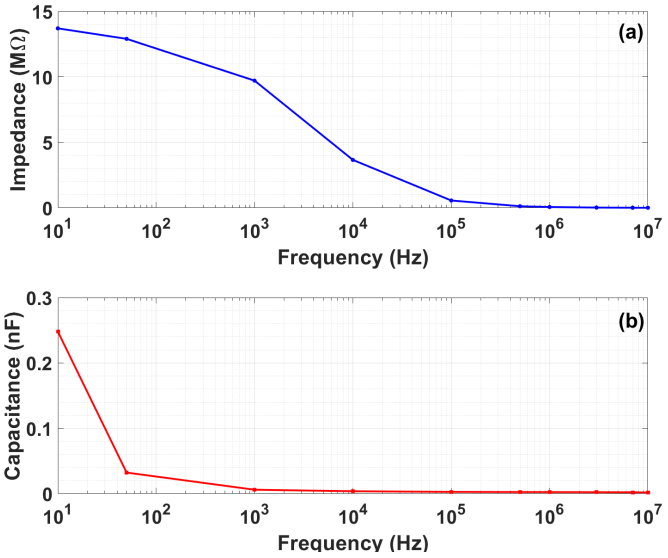

Fig. 8. LCR meter Characterization of the Ag-hBN Sensor. (a) Impedance vs Frequency, and (b) Capacitance vs Frequency

$$|Z(f)| = \frac{1}{2\pi f C_{\text{int}}} \quad \text{for} \quad f < f_c \tag{1}$$

where C_{int} is the interfacial capacitance and f_c ($\sim 10^5$ Hz) indicates resistive dominance. The capacitance remains stable at $0.2 \pm 0.1 \times 10^{-9}$ F below 10 kHz, demonstrating hBN's dielectric consistency, with a decrease beyond 100 kHz due to parasitic inductance. These results confirm the sensor's optimal operation in the 0.1–10 kHz biological frequency range.

COMSOL Multiphysics® simulations modeled the electric field modulation mechanism. The hBN interface concentrated most of the E field within the active sensing region compared to Ag-only, reducing fringe field losses. Fig. 9 presents the electric field distribution within the interdigitated electrode structure of the breathing sensor. The left image corresponds

to the configuration using only silver (Ag) electrodes, while the right image incorporates a hBN interfacial layer at the electrode edges. The introduction of hBN results in a more pronounced concentration of the electric field.

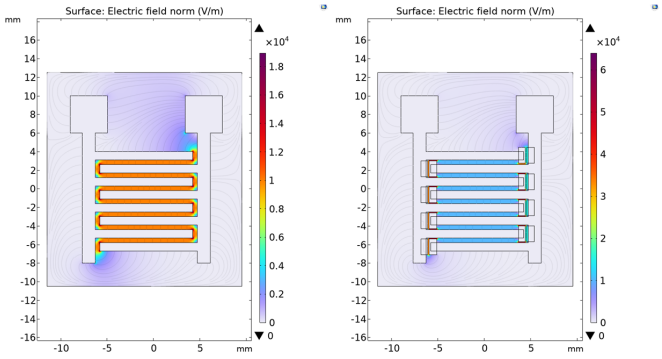

Fig. 9. Electric field distribution of the iJP sensor with only Ag (left) and with hBN added in the interfacial layer (right).

VI. Conclusion

This work demonstrates an inkjet-printed Ag-hBN respiratory sensor that combines cost-effective fabrication ($2.25/unit) with enhanced performance through engineered hBN interfaces. The sensor achieves greater sensitivity than pure Ag electrodes, enabled by the anisotropic dielectric properties of hBN, while maintaining operation below 25 μW power consumption. Robust mechanical stability and distinct responses to breathing patterns validate its potential for wearable health monitoring. The hybrid fabrication approach—combining inkjet-printing with drop-cast hBN patterning—balances precision with scalability. Future development will focus on polymer encapsulation for environmental protection and integration with wireless systems to address current limitations in long-term durability for continuous monitoring scenarios.

Acknowledgment

This work was supported by the USA National Science Foundation (NSF) under Grant No. ECCS-2430440. Any opinions, findings, conclusions, or recommendations expressed in this material are those of the author(s) and do not necessarily reflect the views of the National Science Foundation.

References

[1] V. Patel, A. Orchanian-Cheff, and R. Wu, "Evaluating the validity and utility of wearable technology for continuously monitoring patients in a hospital setting: systematic review," *JMIR mHealth and uHealth*, vol. 9, no. 8, p. e17411, 2021.

[2] S. Majumder, T. Mondal, and M. J. Deen, "Wearable sensors for remote health monitoring," *Sensors*, vol. 17, no. 1, p. 130, 2017.

[3] Y. Khan, A. Thielens, S. Muin, J. Ting, C. Baumbauer, and A. C. Arias, "A new frontier of printed electronics: flexible hybrid electronics," *Advanced Materials*, vol. 32, no. 15, p. 1905279, 2020.

[4] Y. Gao, T. Xiao, Q. Li, Y. Chen, X. Qiu, J. Liu, Y. Bian, and F. Xuan, "Flexible microstructured pressure sensors: design, fabrication and applications," *Nanotechnology*, vol. 33, no. 32, p. 322002, 2022.

[5] G. Liu, Y. Tang, A. M. Soomro, P. Shen, S. Lu, Y. Cai, H. Wang, Q. Yang, H. Chen, Y. Shi *et al.*, "Vertically aligned zno nanoarray directly orientated on cu paper by h-bn monolayer for flexible and transparent piezoelectric nanogenerator," *Nano Energy*, vol. 109, p. 108265, 2023.

[6] M. Zeng, D. Zavanelli, J. Chen, M. Saeidi-Javash, Y. Du, S. LeBlanc, G. J. Snyder, and Y. Zhang, "Printing thermoelectric inks toward next-generation energy and thermal devices," *Chemical Society Reviews*, vol. 51, no. 2, pp. 485–512, 2022.

[7] T. Z. Adry, S. Akter, S. Eliza, S. D. Gardner, and M. R. Haider, "An inkjet-printed flexible memristor device for echo state networks," in *2024 IEEE Computer Society Annual Symposium on VLSI (ISVLSI)*. IEEE, 2024, pp. 740–744.

[8] T. Z. Adry, S. D. Gardner, S. A. Eliza, and M. R. Haider, "A flexible inkjet-printed memristive sensor: Modeling and simulation," in *2024 IEEE 67th International Midwest Symposium on Circuits and Systems (MWSCAS)*. IEEE, 2024, pp. 600–604.

[9] S. D. Gardner, M. R. Opu, and M. R. Haider, "An inkjet-printed capacitive sensor for ultra-low-power proximity and vibration detection," in *2023 IEEE Wireless and Microwave Technology Conference (WAMICON)*. IEEE, 2023, pp. 73–76.

[10] J. Kathirvelan, "Recent developments of inkjet-printed flexible sensing electronics for wearable device applications: a review," *Sensor Review*, vol. 41, no. 1, pp. 46–56, 2021.

[11] S. Akter and M. R. Haider, "mtanh: A low-cost inkjet-printed vanishing gradient tolerant activation function," *Journal of Low Power Electronics and Applications*, vol. 15, no. 2, p. 27, 2025.

[12] R. Lu, M. R. Haider, S. Gardner, J. I. D. Alexander, and Y. Massoud, "A paper-based inkjet-printed graphene sensor for breathing-flow monitoring," *IEEE Sensors Letters*, vol. 3, no. 2, pp. 1–4, 2019.

[13] K. Rajan, I. Roppolo, A. Chiappone, S. Bocchini, D. Perrone, and A. Chiolerio, "Silver nanoparticle ink technology: state of the art," *Nanotechnology, science and applications*, pp. 1–13, 2016.

[14] H. Johnston, G. Pojana, S. Zuin, N. R. Jacobsen, P. Møller, S. Loft, M. Semmler-Behnke, C. McGuiness, D. Balharry, A. Marcomini *et al.*, "Engineered nanomaterial risk. lessons learnt from completed nanotoxicology studies: potential solutions to current and future challenges," *Critical reviews in toxicology*, vol. 43, no. 1, pp. 1–20, 2013.

[15] S. Roy, X. Zhang, A. B. Puthirath, A. Meiyazhagan, S. Bhattacharyya, M. M. Rahman, G. Babu, S. Susarla, S. K. Saju, M. K. Tran *et al.*, "Structure, properties and applications of two-dimensional hexagonal boron nitride," *Advanced Materials*, vol. 33, no. 44, p. 2101589, 2021.

[16] B. A. Vicente, R. Sebastião, and V. Sencadas, "Wearable devices for respiratory monitoring," *Advanced Functional Materials*, vol. 34, no. 45, p. 2404348, 2024.

[17] Y. Lin, C. E. Bunker, K. S. Fernando, and J. W. Connell, "Aqueously dispersed silver nanoparticle-decorated boron nitride nanosheets for reusable, thermal oxidation-resistant surface enhanced raman spectroscopy (sers) devices," *ACS applied materials & interfaces*, vol. 4, no. 2, pp. 1110–1117, 2012.

[18] M. Li, G. Huang, X. Chen, J. Yin, P. Zhang, Y. Yao, J. Shen, Y. Wu, and J. Huang, "Perspectives on environmental applications of hexagonal boron nitride nanomaterials," *Nano Today*, vol. 44, p. 101486, 2022.

[19] Y. Zhang, Q. Lu, J. He, Z. Huo, R. Zhou, X. Han, M. Jia, C. Pan, Z. L. Wang, and J. Zhai, "Localizing strain via micro-cage structure for stretchable pressure sensor arrays with ultralow spatial crosstalk," *Nature Communications*, vol. 14, no. 1, p. 1252, 2023.

[20] E. MacDonald and R. Wicker, "Multiprocess 3d printing for increasing component functionality," *Science*, vol. 353, no. 6307, p. aaf2093, 2016.

[21] A. Kamyshny and S. Magdassi, "Conductive nanomaterials for 2d and 3d printed flexible electronics," *Chemical Society Reviews*, vol. 48, no. 6, pp. 1712–1740, 2019.

[22] L. Nayak, S. Mohanty, S. K. Nayak, and A. Ramadoss, "A review on inkjet printing of nanoparticle inks for flexible electronics," *Journal of Materials Chemistry C*, vol. 7, no. 29, pp. 8771–8795, 2019.

[23] M. A. Shah, D.-G. Lee, B.-Y. Lee, and S. Hur, "Classifications and applications of inkjet printing technology: a review," *IEEE Access*, vol. 9, pp. 140 079–140 102, 2021.

[24] X. Wang, M. Zhang, L. Zhang, J. Xu, X. Xiao, and X. Zhang, "Inkjet-printed flexible sensors: From function materials, manufacture process, and applications perspective," *Materials Today Communications*, vol. 31, p. 103263, 2022.